

Analysis of leakage and diffusion of R290 in the engine compartment of electric vehicle

Xiwen Wang¹², Kuining Li^{12*}, Jiangyan Liu¹², Yi Xie³

1 Key Laboratory of Low-Grade Energy Utilization Technologies and Systems, Chongqing University, Ministry of Education, Chongqing, 400044, China

2 School of Energy and Power Engineering, Chongqing University
Chongqing, 400044, China

3 School of College of Mechanical and Vehicle Engineering, Chongqing University
Chongqing, 400044, China

(*Corresponding Author: leekn@cqu.edu.cn)

ABSTRACT

As an alternative refrigerant of R134a, natural refrigerant R290 has gradually been studied in the automotive air conditioning system. Due to its explosive characteristics, a certain safety hazard will be caused once leaks. This article studies the leakage and distribution of R290 under different working conditions through numerical simulation. The effects of leakage pores, charge amount, and leakage positions on R290 leaked diffusion. The results show that the leakage phase can be divided into a fast leakage stage, buffer stage, and diffusion phase. The leakage of the condenser is the most dangerous situation in the engine compartment leakage. Increasing the aperture and charge will increase the combustible area and duration of R290 leakage. Compared with the leakage diameter, the charge amount is more impact on the continuous duration of the internal flammable areas in the engine compartment.

Keywords: Automotive Air conditioning, R290 refrigerant, leakage diffusion, numerical simulation

NONMENCLATURE

Abbreviations

HFC	High-frequency current
GWP	Global warming potential
LFL	Lower flammable limit

Symbols

ρ	Density of the fluid, kg/m^3
u_i	Velocity component
p	Pressure on the fluid element, Pa
μ	Dynamic viscosity, $\text{Pa} \cdot \text{s}$
f	Unit mass force vector, m/s^2
E	Total internal energy, J
k	Thermal conductivity
T	Temperature, K
h_i	Enthalpy of component i , J/kg
J_i	Diffusion flux, $\text{kg}/(\text{m}^2 \cdot \text{s})$
ϕ	Energy dissipation term, $\text{J}/(\text{m}^3 \cdot \text{s})$
S_h	Energy source term, $\text{J}/(\text{m}^3 \cdot \text{s})$
m_i	Mass concentration of each component of the mixed gas
S_i	Mass source term of component i

1. INTRODUCTION

Since the 21st century, the extreme climate change caused by global warming has become increasingly prominent. Reducing greenhouse gas emissions and reducing greenhouse effect has become an important scientific issue that needs to be solved urgently by the global scientific community. In recent years, countries around the world have signed and introduced a number of conventions and laws aimed at controlling greenhouse gas emissions. Therefore, the search for a new type of environmentally friendly refrigerant has become a very urgent task. As a refrigerant used in air conditioners,

R290 has certain advantages in performance compared with R22[1-4]. Huang [5] built a performance test platform to verify the feasibility and superiority of the water-cycle electric vehicle heat pump air conditioning system based on R290 refrigerant. Compared with R134a and CO₂, R290 has better and more stable heat pump system performance in cold climates. In general, however, HFC-free and low-GWP refrigerants are flammable and face barriers to widespread use due to industry standards. Considering the risk of flammable refrigerant leakage, the current research on flammable refrigerant leakage mainly focuses on the numerical model of leakage diffusion and indoor safety evaluation.

Quanyi Liu et al. [6] regarded the leakage of gaseous refrigerant R290 from the throttle or gap as a natural jet. The results show that the greater the leakage speed, the larger the indoor dangerous area will be, the influence of room size on diffusion is not obvious, and the greater the number of air changes can significantly reduce the risk of R290 leakage. Li et al. [7] tested the safety implications of using R-290 by assessing the effect of certain variables on the concentration of refrigerant leaking into the room. R290 has been leaking under different conditions and its distribution in the room has been measured. Hu et al. [8] studied the dispersion characteristics of refrigerants under different conditions through experiments and simulations. The effects of installation height, leakage point position, airflow velocity and Angle were tested and analyzed. Air volumes with velocities greater than 0.2m/s can be directly used to assess the effect of air flow on refrigerant mixing and diffusion. Jin [9] et al. analyzed the effects of fan speed, leakage point and mechanical ventilation on the diffusion of leakage R32 through experiments, and found that the position near the leakage hole had a high risk, and fan speed and mechanical ventilation contributed to the diffusion of leakage R32. Tang et al. [10] conducted an experimental study on the risk of air source heat pump R290 after leakage. The results show that during the whole leakage process, combustible zone continuously appears in the inner region of the air source heat pump. But outdoors, it only appears around the source heat pump and in areas very close to the ground. Wu [11] found that ventilation is an effective way to improve the leakage safety of R290. The leak hole diameter has an overwhelming effect on the concentration distribution of R290. The closer you are to the leak, the higher the concentration. In heating conditions, except for the part of the air supply outlet directly below the leak point, the indoor area is generally safe. Tang [12] found that under the steady-state refrigeration mode, most of the

refrigerant (72-80%) is concentrated in the outdoor unit. In the event of an indoor leak, the combustible area appears only below the leak location in the sealed room. When the leak hole is 0.5 mm, the combustible zone range and residence time increase with the amount of refrigerant charged, and the indoor fire risk can be ignored.

According to current researches on R290 leakage, most of them focus on indoor air conditioning systems and heat pump systems, while automotive air conditioning systems have more variable working conditions and environments. Therefore, this paper studies the leakage and diffusion of R290 in the automotive engine compartment through numerical simulation.

2. LEAKAGE NUMERICAL SIMULATION

2.1 Mathematical model

The governing equations of refrigerant leakage and diffusion include continuity equation, momentum conservation equation, energy conservation equation and component transport equation. The governing equations are as follows:

Continuity equation:

$$\frac{\partial \rho}{\partial \tau} + \nabla \cdot (\rho \mathbf{u}_i) = 0 \quad (1)$$

Where ρ is the density of the fluid, kg/m³;

u_i is the velocity component in the x, y, and z directions, m/s.

Momentum conservation equation:

$$\rho \left(\frac{\partial u_i}{\partial \tau} + u \nabla u \right) = -\nabla p + \mu \nabla^2 u + \rho f \quad (2)$$

Where p is the pressure on the fluid element, Pa;

μ is the dynamic viscosity, Pa · s; f is the unit mass force vector, m/s².

Energy conservation equation:

$$\frac{\partial(\rho E)}{\partial \tau} + \nabla[u(\rho E + p)] = k \nabla^2 T - \sum_i h_i J_i + \phi + S_h \quad (3)$$

Where E is the total internal energy, J;

k is the thermal conductivity;

T is the temperature, K;

h_i is the enthalpy of component i, J/kg;

J_i is diffusion flux, kg/(m² · s);

ϕ is the energy dissipation term, J/(m³ · s);

S_h is the energy source term, J/(m³ · s).

Component transport equation:

$$\frac{\partial(\rho m_i)}{\partial \tau} + \nabla(\rho u m_i + J_i) = S_i \quad (4)$$

Where m_i is the mass concentration of each component of the mixed gas;

S_i is the mass source term of component i .

2.2 Basic assumption

The numerical simulation of the gas leakage diffusion process is very difficult, in the simulation of the process needs to simplify the simulation of the mathematical model, in order to reduce the requirements of the computer, so that the calculation results are easier to converge, the following basic assumptions and simplification.

Basic assumptions of the model:

(1) The air in the engine compartment is an incompressible fluid, and the leakage process is turbulent.

(2) Since the refrigerant will instantly vaporize and expand when it leaks into the atmospheric space under high pressure, it is considered that the leakage of R290 refrigerant is a gas leak, and R290 refrigerant does not react chemically with the indoor air, and the mixture of R290 and air is regarded as an ideal gas, and the ideal gas equation of state is applicable.

(3) In atmospheric environment, the effect of height on gravitational acceleration is ignored and considered as a constant value;

The boundary conditions for engine compartment leakage diffusion simulation analysis are shown in Table 1.

Table 1

Boundary condition	
Name	Setting
Leakage inlet	Mass flow inlet
Outlet	Pressure outlet
Radiator, condenser	Resistance model of porous media
Fan	Slip grid

2.3 Basic assumption

In this paper, the three-dimensional model of the engine compartment is constructed. Due to the large number of components in the engine compartment, appropriate correction and simplification are carried out in the simulation. The processed model is shown in Fig 1. To monitor the dynamic volume concentration distribution of refrigerant in the engine compartment, four concentration monitoring points are set up.

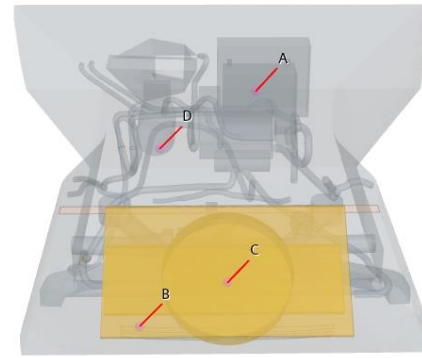


Fig. 1 Simplified model of engine compartment

2.4 Operating parameter

The initial conditions for setting the vehicle CFD model are as follows

(1) The internal and external pressure of the engine room is the environmental pressure of 101325Pa (gauge pressure is 0).

(2) The engine compartment air group is 100%.

(3) The leakage pressure is 1.5MPa.

To assess the impact of various factors, the following test conditions were selected, as shown in Table 2.

Table 2

Working condition		
Leakage location	Aperture(mm)	Charge amount
Condenser/Compressor	2/4/7	250g/500g

3. RESULTS AND ANALYSIS

3.1 Effect of different leak apertures

Refrigerant leakage is a dynamic process. Different leakage rates and pressures of R290 under different leakage diameters are depicted based on the calculation process, as shown in Fig 2. Taking the leakage aperture of 7mm as an example, it can be seen from the figure that R290 has a faster leakage speed in the initial stage. With the increase of time, the R290 concentration in the engine compartment increases, the R290 mass inside the system gradually decreases, the system pressure decreases, the internal and external pressure difference decreases, and the leakage mass flow rate at the leak hole gradually decreases. According to the calculation results, the leakage mass flow rate of R290 at the initial time is 0.127kg/s, the leakage flow rate decreases to 0.0004kg/s in 7s, and the leakage amount is almost zero after 8s.

Fig. 3 shows the concentration distribution at $x=0.85m$ (the leak plane) for different apertures when leaking for 1 second. From the graph, we can observe

that propane is jetted out from the leak orifice with a high velocity, resulting in horizontal movement. Due to the obstruction of the condenser and radiator, some gas diffuses upward at the front end of the jet. As the orifice size increases, the diffusion range of propane inside the engine compartment becomes larger for the same leakage time.

The distribution of the working medium concentration at point B is plotted as the curve shown in Fig 4. As can be seen from Fig 4, the concentration curves under different pore sizes are similar, mainly divided into three stages, namely, the rapid leakage stage, the buffer stage, and the diffusion stage. R290 will rise for a short period of time, then decline and stabilize, which is due to inertia. The leakage rate of refrigerant at the beginning is very high, which is also the reason for the rapid increase in R290 concentration during the rapid leakage stage. Subsequently, the leakage rate began to moderate, resulting in a process of R290 decreasing and then increasing during the buffering phase. The final stage of the leakage process is the diffusion stage, when most of the R290 refrigerant has leaked out of the system and the pressure inside the system gradually decreases. At this point, the leakage rate also gradually

decreases and begins to be lower than the diffusion rate of R290 in the engine compartment. Therefore, the concentration of R290 in the engine compartment began to slowly decrease and gradually stabilize.

In order to compare the effects of different pore sizes, the concentration data at points B and C were compared, and the results were shown in Table 3. Obviously, the maximum concentration of each point under different aperture is different, and the smaller the aperture, the lower the maximum concentration corresponding to the same position. And by calculating the leakage flow corresponding to the time of reaching the highest concentration, basically around 0.0015kg/s. By comparing the duration of each point concentration above LFL under different aperture, it can be seen that the larger the aperture, the longer the R290 stays in the combustible area of the engine compartment. The reason for this is that the larger the leakage aperture, the greater the corresponding leakage velocity. However, the leakage flow at a 2mm leak aperture was sufficient to cause R290 concentrations in the two monitoring points in the engine compartment to exceed LFL. And its leakage duration is longer, under the action of longer leakage time, the duration of the combustible region

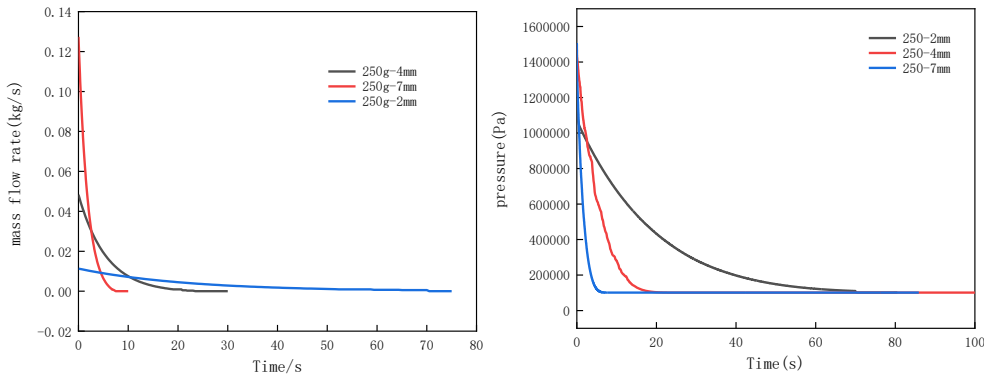


Fig. 2. The change curve of leakage flow and pressure with time under different apertures

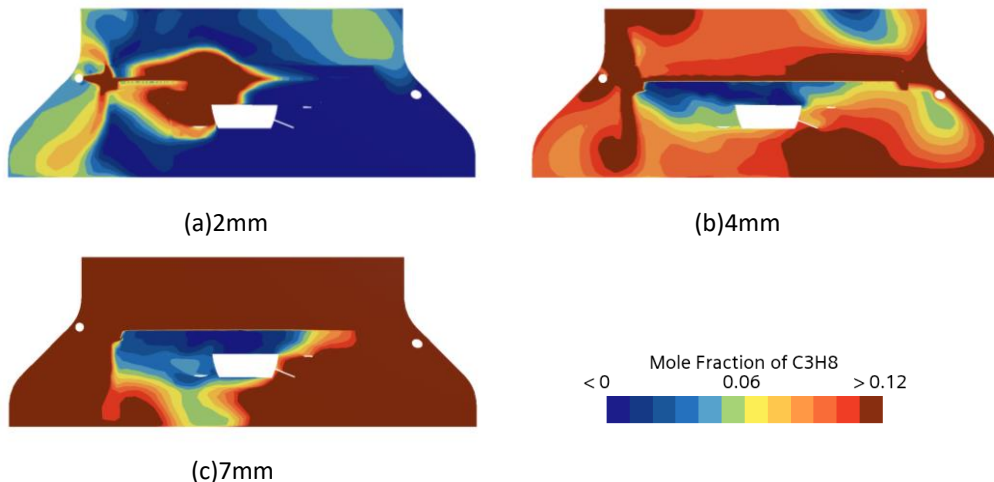


Fig. 3 Cloud map of concentration distribution at t=1s at different apertures

under the leakage aperture of 2mm is longer than that of the leakage aperture of 4mm.

By comparing the highest concentration at each point, it can be seen that when the aperture is 2mm and 4mm, the concentration at point B is greater than that at point C, but it is different when the aperture is 7mm. This is because when the aperture is small, R290 leaks into the engine room, due to the action of gravity, point B is closer to the plume axis, so the concentration is higher.

Table 3

Concentration data at different apertures

Aperture	Position	Concentration of R290	Duration above LFL level
2mm	B	15.62	951.19
2mm	C	13.37	1039.11
4mm	B	19.66	926.5
4mm	C	17.45	1027.41
7mm	B	17.79	981.81
7mm	C	20.1	1047.36

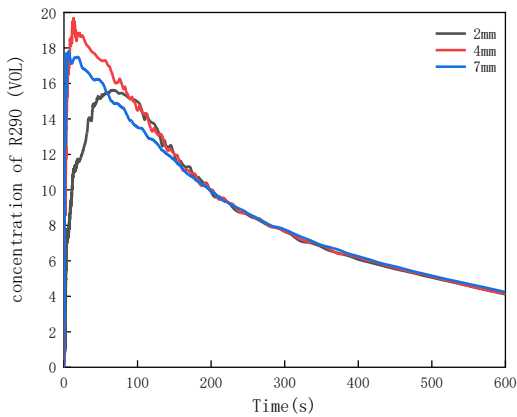


Fig. 4 Concentration distribution of different apertures at point B

3.2 Effect of different refrigerant charge

According to the calculation, the change curve of R290 leakage flow rate with time when the leakage aperture is 4mm at different charging amounts is drawn, as shown in Fig 5. It can be seen from the figure that the flow curves of different charging volumes are similar. When the charging volume is 250g, the leakage time is about 20s, and when the leaking time is about 43s for 500g.

The concentration distribution of working medium at measuring point B is drawn as a curve as shown in Fig 6. It can be seen from Fig 6. that at the initial stage of leakage with different charge curves, the concentration at this point changes almost the same with time.

However, due to different charge amounts, the leakage time increases, resulting in an increase in the

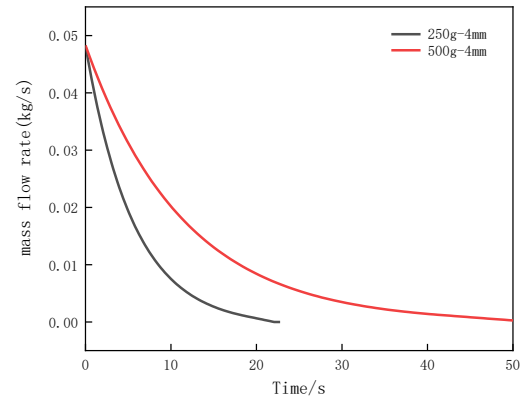


Fig. 5 Change curve of leakage flow with time under different charging amount

duration and maximum concentration of R290 in the engine compartment, and an increase in the ignition risk in the engine compartment. The combustible zone duration is 962.59s at 250g of charge, and increases to 1180.35s at 500g. In addition, compared with different apertures, the change of charge volume has a greater effect on the duration of combustible zone in the engine compartment.

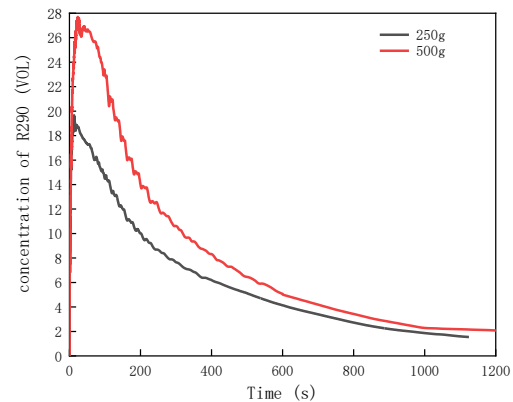


Fig. 6 The concentration distribution of different charge amounts at point B

3.3 The effect of different leak locations

The condenser leak is located at the front of the engine compartment, and the compressor leak is located at the middle and back end of the engine compartment. Fig 7. shows the concentration distribution at $y=0$ (the center position of the engine compartment) at different leakage positions for 1s of leakage. It can be seen from the figure that R290 in the early stage of propane leakage from the condenser is mainly concentrated in the front of the engine room, and R290 in the early stage of compressor leakage is mainly concentrated in the middle and upper part of the engine room, which is caused by different leakage positions. The concentrations of each

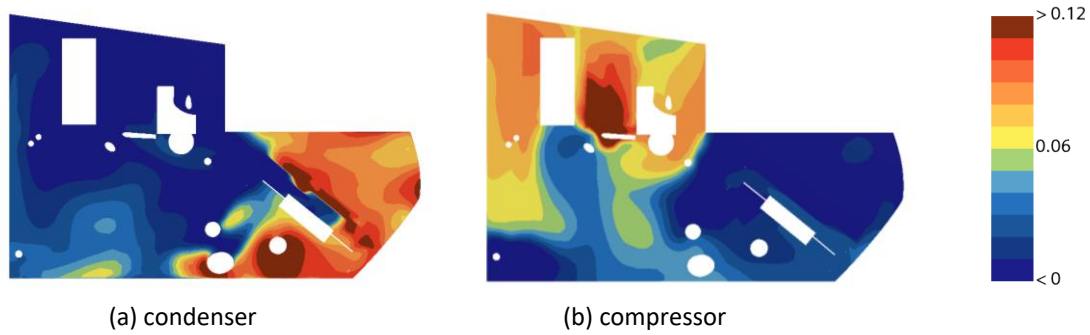


Fig. 7 Cloud map of concentration distribution at $t=1s$ at different leakage locations

point at different leakage locations are shown in Table 4. It can be seen from the table that when the compressor leaks, the R290 combustible zone duration is significantly lower than that of the condenser leakage. Since the engine compartment is a semi-enclosed space, there is air circulation behind the engine compartment, which will cause the compressor to leak, most of the R290 accumulates in the rear of the engine compartment, and quickly exits the engine compartment under the dilution of air, thereby reducing the duration of the combustible area.

Table 4

Concentration data at different leak locations

Leakage location	Position	Concentration of R290	Duration above LFL level
Condenser	A	14.28	569.04
Condenser	B	19.66	926.5
Condenser	C	17.45	1027.41
Condenser	D	17.15	840.58
Compressor	A	17.224	520.83
Compressor	B	14.14	798.41
Compressor	C	12.447	665.24
Compressor	D	18.85	533.61

As can be seen from Fig. 3 And Fig. 7, R290 will have a small area of high concentration on both sides of the engine compartment, and there will also be a gathering phenomenon near the ground. This is because R290 can not continue to move when it hits the wall during diffusion. According to relevant knowledge of fluid mechanics, after the fluid hits the wall, some of the fluid will move in other direction due to "rebound", but a large part of the fluid will stop here, transform the kinetic energy into pressure energy and potential energy, and react on the flowing fluid to balance the driving force of the incoming flow. This also explains the greater risk of combustion of a condenser leak compared to a compressor leak when an electric vehicle is stationary.

4. CONCLUSION

The amount of refrigerant charged in the heat pump air conditioning system of new energy electric vehicles is significantly higher than that of traditional fuel vehicles, and the risk assessment is of great significance when using combustible refrigerants. In this paper, the volume concentration distribution and safety of flammable and explosive refrigerant R290 after leakage in the engine compartment of electric vehicle were numerically simulated and analyzed, and the following conclusions were obtained:

(1) When R290 leaks, the leakage rate is the largest in the initial stage, and the leakage rate increases with the increase of the leakage aperture, and the effective leakage time decreases with the increase of the leakage aperture.

(2) The concentration curve of the leakage stage is similar, which is mainly divided into three stages, namely, the rapid leakage stage, the buffer stage, and the diffusion stage.

(3) The increase of leakage aperture and charge volume will increase the combustible area and duration in the engine compartment when R290 leaks. Compared with the leakage aperture, the change of charge volume has a greater impact on the duration of combustible area in the engine compartment.

(4) Compared with compressor leakage, condenser leakage is the most dangerous situation for R290 in the engine compartment.

DECLARATION OF INTEREST STATEMENT

The authors declare that they have no known competing financial interests or personal relationships that could have appeared to influence the work reported in this paper. All authors read and approved the final manuscript.

REFERENCE

- [1] Shaik V S ,Setty P T B A.Thermodynamic Analysis of Window Air Conditioner Using Sustainable Refrigerant R290/RE170 and R1270/RE170 Blends as Substitutes to Refrigerant R22[J].International Journal of Heat and Technology,2019,37(1):80-94.
- [2] Choudhari C ,Sapali S .Performance Investigation of Natural Refrigerant R290 as a Substitute to R22 in Refrigeration Systems[J].Energy Procedia,2017,109346-352.
- [3] Padmanabhan V M V ,Palanisamy K S .Exergy efficiency and irreversibility comparison of R22, R134a, R290 and R407C to replace R22 in an air conditioning system[J].Journal of Mechanical Science and Technology, 2013, 27(3): 917-926.
- [4] Yun Z ,Cichong L ,Wanyong L , et al.Performance and Optimization Study of R290 as Alternative Refrigerant for R22 in Low Temperature Heat Pump System[J]. Journal of Physics: Conference Series,2021, 2108(1):
- [5] Yue H ,Xiuchun W ,Jiahao J .Research on the electric vehicle heat pump air conditioning system based on R290 refrigerant[J].Energy Reports,2022,8(S7):447-455.
- [6] Liu Q ,Zhang H ,Liu Y , et al.Influencing Factors of Flammable Refrigerants Leaking in Building Air-conditioning System[J].Procedia Engineering, 2013, 62648-654.
- [7] Li T .Indoor leakage test for safety of R-290 split type room air conditioner[J].International Journal of Refrigeration, 2014,40380-389.
- [8] Maojuan H ,Jinbo L ,Zhe L , et al.Experimental and numerical simulation analysis of R-290 air conditioner leak[J].International Journal of Refrigeration, 2018, 90163-173.
- [9] Jin W ,Gao P ,Zheng Y .Experimental Study on Ventilation Effect on Concentration Distribution of R32 Leaking from Floor Type Air Conditioner[J].Energy Procedia,2017,1054627-4634.
- [10] Tang W ,He G ,Zhou S , et al.The performance and risk assessment of R290 in a 13 kW air source heat pump[J].Applied Thermal Engineering,2018,144392-402.
- [11] Wu G ,Ma G ,Xu S , et al.Experimental study of leakage safety of a novel integral-type air conditioner using R290[J].International Journal of Refrigeration,2022,144296-304.
- [12] Tang W ,He G ,Zhou S , et al.The experimental study of R290 mass distribution and indoor leakage of 2 HP and 3 HP split type household air conditioner[J]. International Journal of Refrigeration, 2019, 100246-254.